SMGroup

SM Journal of Biometrics & Biostatistics

Research Article

Statistical Analysis and Inter-Comparison of Linke Turbidity Factor for Two Sites in Cyprus: Athalassa (Inland Location) and Larnaca (Coastal Location)

Pashiardis S[1], Kalogirou SA[1]* and Pelengaris A[2]

[1]*Department of Mechanical Engineering and Materials Science and Engineering, Cyprus University of Technology, Cyprus*

[2]*Department of Cyprus Public Works, Ministry of Transport Communications and Works, Cyprus*

Article Information

Received date: Apr 11, 2018
Accepted date: Apr 20, 2018
Published date: Apr 26, 2018

***Corresponding author**

Kalogirou SA, Department of Mechanical Engineering and Materials Science and Engineering, Cyprus University of Technology, Limassol, Cyprus,
Tel: +357-2500-2621;
Fax: +357-2500-2637;
Email: soteris.kalogirou@cut.ac.cy

Keywords Atmospheric turbidity; Linke turbidity factor; global radiation; statistical analysis; turbidity parameters; Cyprus

Abstract

Hourly global and diffuse irradiance data are used to estimate Linke turbidity factor (T_L) at two sites in Cyprus, representing two different climate regimes of the island (Athalassa-inland plain *vs* Larnaca-coastal location) for the period January 2013-December 2015. The annual mean values of T_L are 3.40 at both stations. The daily and monthly variation of atmospheric turbidity has been studied. It was found that atmospheric turbidity decreases during the winter season (rainy season) and increases during the summer season. The higher diurnal variation is observed in spring and summer months at both stations. T_L is increased from morning to afternoon. The increase of T_L from morning to afternoon can be attributed to the fact that higher traffic activities are observed during the day at both stations. The results presented are comparable to those recorded in different places in Mediterranean region. The Cumulative Frequency Distributions (CDF) of T_L shows that about 37% of T_L values are less than 3, 50% are between 3 to 5 and only 13% are greater than 5. This indicates that the skies on cloudless days are clean and clear. The short-term variation of atmospheric turbidity depends on local weather conditions (temperature, vapour pressure, wind speed and wind direction) and its long-term one on the climate of the area. It was found that the Linke turbidity factor is increased linearly with air temperature at both stations. T_L is also increased with increasing the vapour pressure at both stations. The prevailing winds, which may transport moisture or aerosol particles from distant sources, play a major role in the spatio-temporal variation of turbidity. Wind speed also plays a significant role in the transport of moisture or aerosol particles. The diffuse irradiance is increased with the increase of atmospheric turbidity. Linear relationships were established between diffuse irradiance and atmospheric turbidity. Comparing T_L values of different locations over the island, it was found that the high altitude station has the lowest values, since this station has clearer atmosphere than the other sites.

Introduction

The sun's radiation, as it passes through the atmosphere, gets attenuated by the constituent gases, suspended particles (aerosols) and clouds. Solar radiation is attenuated by absorption and scattering processes; the main gaseous absorbers are ozone, oxygen, water vapour and carbon dioxide. Absorption by the molecules and the atoms takes place in discrete wavelengths. However, all atmospheric gases and aerosols scatter solar radiation at all wavelengths, although absorption by aerosols is smaller than by scattering. Under cloudless conditions, ozone, water vapour and aerosols are the most important atmospheric components affecting solar radiation. The amount of aerosols and their physical properties are important characteristics of atmospheric pollution, giving valuable information on the values of diffuse and beam solar radiation [1].

An aerosol is a solid or liquid particle with 10^{-3} to 10^{2} μm radius and it follows the motion of air within certain broad limits [2]. These particles are either of terrestrial origin (industrial smoke, pollen, volcanic eruptions, sandstorms, forest fires and agricultural burnings), or of maritime origin (salt crystals, ocean spray and nuclei of hydroscopic salt on which water has condensed). Aerosols play a role in the earth's energy balance, in cloud formation, precipitation and in atmospheric chemical reactions. An atmosphere with aerosols is called turbid and the effects that those aerosols produce on solar radiation are known as turbidity [3]. Assessing the magnitude and temporal variability of turbidity is important for a variety of applications such as agronomy, climate modelling, solar energy production and the control of air pollution [4-6].

The turbidity of the atmosphere, in a cloud-free atmosphere, is expressed by an index of turbidity. The most commonly used coefficients are the Ångström turbidity coefficient β and the Linke turbidity factor T_L [1,7-13]. The Linke turbidity factor represents the turbidity caused by aerosols and water vapour, which affects solar radiation by absorption in the visible and near infrared regions. On the

Table 1a: Site parameters for the two meteorological stations for the period 2013-2015.

Site	Location	Latitude	Longitude	Altitude (m,m.s.l)
Athalassa	inland	35.141^{0}N	33.396^0 E	165
Larnaca	coastal	34.873^{0}N	33.631^0 E	1

other hand, the Ångström turbidity coefficient β has been accepted as an index of the turbidity caused by aerosols, as it represents the aerosol amount in the air. The value of β varies typically from 0 to 0.5 [14]. The Linke turbidity factor refers to the whole spectrum, that is, overall spectrally integrated attenuation, whereas the Ångström turbidity coefficient is obtained from spectral measurements. Values of T_L ranging from 1.8 to 2.8 represent very clear atmosphere, while values between 2.4 and 3.9 represent a clear maritime atmosphere. Values of T_L ranging from 3.0 to 4.8 represent an urban atmosphere and values between 3.6 and 6.0 represent an industrial atmosphere [7]. Dogniaux [15] has developed an empirical relationship between T_L and β.

Long-term monthly average values, T_{Lm}, are sufficient for most applications. Several methods for estimating T_{Lm} values can be found in literature: for example from time series of daily global horizontal irradiation (Aguiar, in [16]); from monthly Ångström sum of regression coefficients [7]; from subjective assessments of the type of atmospheric conditions prevailing in the region of interest (linear regression with latitude and with the Atmospheric Turbidity Index [12]. A World Wide Web site "Helioserve" has been established, which offers an access to the database of monthly T_L values through a standard HTML interface.

An assessment of the solar radiation climate of the Cyprus environment was presented by Jacovides [18]. Kambezidis [19] presented the 'Typical Meteorological Year' for Nicosia, whereas Kalogirou [20] presented the TMY-2 for the same location. More recently, Kalogirou et al. [21] presented a statistical analysis and inter-comparison of the solar global radiation at the above two sites in Cyprus using measurements of 21 months at both sites. The common feature of all the above studies is that they rely mostly on measurements of solar radiation carried out in the actinometric stations of Athalassa and Larnaca.

T_L can be estimated either directly through the beam normal irradiance which is measured by pyrheliometer or indirectly through the measurements of global and diffuse irradiance on a horizontal surface, which are performed with pyranometers. In the present study, the hourly beam irradiance is estimated from the difference of diffuse from global irradiance measurements, using data from two locations in Cyprus, representing two different climate regimes (inland *vs* coastal) and covering the period 2013-2015. Furthermore, the method was extended by estimating the diffuse irradiance from the relationship of the fraction of diffuse to global irradiance as given by Jacovides et al. [22]. This is the first time that atmospheric turbidity is estimated for a number of locations over the island, representing different climates. The method was also implemented for a number of stations distributed all over the island, using hourly global solar irradiances measurements during the period 2000-2010. The diurnal and monthly variation of T_L was investigated for the two locations and their frequency distribution was calculated. The correlation of various meteorological parameters with the Linke turbidity factor is also analyzed and discussed. The T_L values were also compared with other sites in the Mediterranean region.

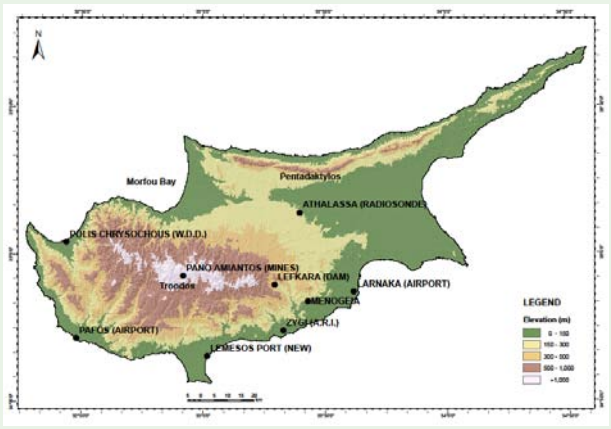

Figure 1: Map of Cyprus showing the location of all the radiometric stations.

Topography, climatology, measurements and quality control

Topography and climate characteristics of the two sites

The radiation data on which this study is based are being monitored at two meteorological stations: one located at Athalassa, an inland plain location and the other one at Larnaca Airport which is near the coast (Figure 1). The site parameters of the two stations

Table 1b: Site parameters for the nine meteorological stations measuring solar global radiation and their period of measurements.

Site	Location	Latitude	Longitude	Alt. (m, m.s.l)	Period
Polis	coastal	35.050^0 N	32.433^0 E	20	06/2000-2010
Amiantos	mountainous	34.933^0 N	32.917^0 E	1360	09/2001-2010
Limassol	coastal	34.667^0 N	33.017^0 E	3	07/2000-2010
Mennogia	inland	34.850^0 N	33.433^0 E	140	10/2001-2010
Paralimni	coastal	35.067^0 N	33.967^0 E	70	03/2001-2010
Lefkara Dam	mountainous	34.900^0 N	33.300^0 E	420	07/2000-2010
Zygi	coastal	34.750^0 N	33.333^0 E	40	10/2009-2010
Athalassa	inland	35.150^0 N	33.396^0 E	165	08/2000-2010
Pafos A/P	coastal	34.783^0 N	32.483^0 E	8	10/2004-2010

are listed in Table 1a. The calculation method of the Linke Turbidity Factor was also extended by estimating it from the global hourly horizontal irradiance, which is a quantity measured by means of a pyranometer. For this purpose hourly global solar irradiance data for nine stations have been used. The covering period of measurements is about 10 years. The site parameters of the nine stations are listed in Table 1b including the recording period of each station. The first number in the column of the period is the starting month.

The climate of both stations is typical Mediterranean with mild winters (mean seasonal air temperature of about 12 °C at Larnaca and 10.5 °C at Athalassa) and warm summers (mean seasonal air temperature of 27.5 °C at Larnaca and 29.5 °C at Athalassa). At Larnaca Airport sea-breeze cells develop in late spring and summer. Although Athalassa is an inland location, a westerly sea-breeze is mainly noticeable during the summer time blowing from the Morphou bay between the mountainous ranges of Pentadactylos and Troodos (Figure 1). The annual rainfall is about 320 mm at Athalassa and about 340 mm at Larnaca. Most of the rainfall occurs between October and March; summer months are mostly dry. The two sites are characterised by relatively high global and horizontal beam radiation intensities. The average annual sunshine duration is 3332 hours for Athalassa and slightly higher at Larnaca (3368 h). All the above climatic averages refer to the 1981-2010 period.

The annual average daily global radiation exceed 18.5 MJ m^{-2} at the two sites, whereas the horizontal beam radiation is 13.1 MJ m^{-2} for Athalassa and 14.2 MJ m^{-2} for Larnaca, respectively. Consequently, the fraction of the beam component of the global radiation is relatively high at both sites, viz., the annual average daily fraction is >0.600 at the two sites. Comparing the two sites it seems that Larnaca has slightly higher rates of global radiation than Athalassa, since the average yearly cumulative global irradiation is 6835 MJ m^{-2} for Athalassa and 7183 MJ m^{-2} for Larnaca. The monthly average frequency of days according to the classification of the magnitude of the daily clearness index K_T (daily global to daily extraterrestrial radiation), showed that both clear and partially cloudy days exceed 90% annually (K_T>0.35) [21].

Measurements and quality control processes

The period for presenting the data in both stations is January 2013 until December 2015 (i.e., 3 years), when both stations operated simultaneously, so as to allow for comparison of the different variables of solar and terrestrial radiation. The global and diffuse radiation components are measured with CM6B Kipp&Zonen pyranometers (First class instruments) at Athalassa, while at Larnaca CMP11 pyranometers (Secondary standard) are used. The direct normal irradiance is measured with a pyrheliometer CH1 at Athalassa and at Larnaca the new model of the pyrheliometer is installed (CHP1, First class pyrheliometers) obtained both from Kipp&Zonen company. Both stations have fully automatic sun tracker systems (2AP at Athalassa and Solys 2 at Larnaca). All the sensors are factory calibrated, in accordance with the World Radiometric Reference (WRR). Global radiation instruments are calibrated outdoor against standard references at irregular time intervals during the study period. The errors involved in the radiation measurements are found to be no less than ±2% for the normal incidence beam irradiance and ±3% for the global irradiance.

A Campbell Scientific Instruments data-logger, located at each site (Model CR10), monitors and stores the data at 10-min intervals (the meters are scanned every 10-seconds and average, maximum, minimum and instantaneous values at 10-min intervals are calculated and stored). The stored data are downloaded to a desktop computer periodically. The data refer to the Local standard Time (LST=GMT+2). About 5% of the data values are missing because of some problems with the instruments and some defects and maintenance in the data acquisition systems. The validity of the individual measurements was checked in accordance with WMO recommendations [23] and other tests proposed by various authors [24- 26]. Details about the quality control procedures used in this study are given by Pashiardis and Kalogirou [27]. All data that do not meet the conditions specified by the suggested tests are not used in the study.

Mean hourly values of all radiation variables were calculated from the 10 min observations. Since turbidity is an index for comparison of cloudless atmospheric environments, it is important to consider the definition of a clear day condition. Different definitions are used in literature for selecting clear days [28-30]. The criteria are based mainly on the levels of direct normal or diffuse irradiances, the ratio of diffuse to global irradiance, the clearness index (i.e., the ratio of the measured global irradiance on the ground surface (G) to the extraterrestrial irradiance (G_0) both measured on horizontal surfaces) ($k_t = G / G_0$). In this paper the following clear sky criteria are adopted:

- To avoid conditions such as thin haze in early morning or in late afternoon, only the data records for solar elevation (α_s) greater than 7^0 were selected;
- The normal incident direct irradiance (B_n) exceeds 200 W m^{-2}; B_n is estimated from the difference of global (G) and diffuse (D) irradiance divided by the cosine of zenith angle (θ_z):

$$B_n = (G - D) / \cos(\theta_z) \quad (1)$$

- The clearness index (k_t)≥0.65;
- The relative sunshine duration (σ), i.e., the ratio of the hourly measured sunshine duration in minutes to the one hour value (i.e., 60 min) should exceed the value of 0.9.

Clear sky data that satisfy the above criteria were used in this analysis. The selected measurements were made on clear days and thus became a restrictive factor on the number of measurement period during a given month. Table 2 shows the number of records used for the analysis after the implementation of the above criteria for the period of 3 years on a monthly basis. The similarities between the two stations are evident. The total number of records for Athalassa for the estimation of T_L is finally 5625 and slightly higher for Larnaca (6147), since more clear days are expected on this site [21]. The highest number of records is observed during the summer time. Simultaneously with the solar radiation measurements, the wind direction, wind speed, air temperature and the relative humidity were measured and recorded on an hourly basis at each station. Table 3 shows the monthly mean values of each atmospheric parameter for the three years period. The radiation parameters at the two locations are almost similar. However, temperatures during the summer period are higher at Athalassa than at Larnaca, while the opposite is valid for relative humidity. Wind speeds are generally much higher at Larnaca

Table 2: Number of hourly data (N) for the determination of clear days based on the selected criteria for the estimation of Linke turbidity factor during the 3 years period.

	Athalassa				Larnaca			
Month	N(α_s>7^0)	N(B_n>200 W m^{-2})	N(k_t≥0.65)	N(σ>0.9)	N(α_s>7^0)	N(B_n>200 W m^{-2})	N(k_t≥0.65)	N(σ>0.9)
1	744	481	244	222	850	576	284	237
2	828	582	343	309	641	496	321	261
3	953	684	457	416	1041	798	512	442
4	1074	862	582	526	1104	920	654	558
5	914	744	521	490	1221	1011	691	611
6	1134	1022	735	694	1246	1163	839	784
7	1149	1121	825	808	1299	1260	886	864
8	1116	1069	712	695	1205	1161	764	727
9	957	827	530	503	1044	941	627	568
10	903	736	471	445	977	860	567	497
11	674	534	286	259	808	637	331	302
12	710	496	282	258	761	592	344	296
Total	11156	9158	5988	5625	12197	10415	6820	6147

than at Athalassa due to the proximity of the site to the sea. The prevailing wind directions at Larnaca are South-Westerlies during the day and North-Westerlies at night. On the other hand, Westelies are the prevailing directions at Athalassa.

Calculation of Linke turbidity factor

Linke's turbidity factor, T_L, represents the atmospheric turbidity caused by aerosols and water vapour and indicates the number of ideal (clean and dry) atmospheres that produce the same extinction of the extraterrestrial solar beam as the real atmosphere. The value of Linke turbidity factor can be derived simply from data obtained from pyrheliometric measurements [2,5,8-9,11-13,30,32-37] these values normally vary from 1 to 10. High values of the Linke turbidity factor mean that the solar radiations are more attenuated in a clear sky atmosphere.

The Linke's turbidity factor, T_L, is calculated from the following expression which was proposed by Mavromatak is and Franghiadakis, [30]:

$$T_L = T_{LK} \frac{1/\delta_{Ra}(m)}{1/\delta_{RK}(m)} \quad (2)$$

where T_{LK} is the Kasten [38] turbidity factor, $\delta_{RK}(m)$ is the Rayleigh integral optical thickness given by the same author and $\delta_{Ra}(m)$ is the integral optical thickness given by Louche et al. [14] and adjusted by Kasten [39]. This is necessary because Kasten had taken into account only molecular scattering and ozone absorption. Absorption by permanent atmospheric gases was not included into the calculations leading to smaller values of the integral optical

Table 3: Mean monthly values of atmospheric parameters at the two stations for the period 2013-2015.

	Athalassa							Larnaca						
Month	G	D	B(G-D)	Bn	Ta	RH	W	G	D	B (G-D)	Bn	Ta	RH	W
	(W m^{-2})	(W m^{-2})	(W m^{-2})	(W m^{-2})	(^{0}C)	(%)	(m s^{-1})	(W m^{-2})	(W m^{-2})	(W m^{-2})	(W m^{-2})	(^{0}C)	(%)	(m s^{-1})
1	311.5	134.5	177	395.3	10.6	78.1	1.8	285.8	128.5	157.3	390.2	12.7	73.6	3.5
2	368.2	138.8	229.4	459.9	11.4	74.2	1.9	397	143.5	253.5	508.1	13.1	72.3	3.6
3	461	168	293.1	483.4	14.2	63.7	2.4	435.8	158.1	277.7	494.5	15.4	64.6	3.9
4	514.1	166.6	347.6	527.8	17.4	59.5	2.5	528.8	160.8	368	572.1	18	62.3	3.9
5	549.5	169.6	379.8	534.8	22.2	59.3	2.6	548.8	166.9	381.8	554.9	22.1	65.9	3.7
6	557.7	133.7	423.4	603	26.1	51.2	3	585.9	139	446.9	637.4	25.2	63.9	4.3
7	615.5	120.3	495.2	687.3	28.8	52.7	2.7	580.6	120.9	459.7	678.9	27.5	67	4.3
8	573.9	130	443.9	637.3	29.8	53.5	2.5	556.5	125.6	430.9	641.9	28.8	64.7	4
9	488	135.9	352	558.5	26.3	56	2.5	514.7	132.6	382.1	634.5	26.5	60.6	3.8
10	425.7	115.5	307.9	561.8	21.2	57.1	2	422.3	115.1	307.2	643.5	22.3	56	3.4
11	348.1	120.2	227.9	495.7	16.6	64	1.6	335.9	126.1	209.8	517.3	18.5	60.1	3.4
12	297.8	109.5	188.4	458.3	11.8	72.5	1.6	291.3	107.3	184	483.8	14.1	67.6	3.8
Year	459.3	136.9	322.1	533.6	19.7	61.8	2.2	456.9	135.4	321.6	563.1	20.4	64.9	3.8

thickness and consequently, to larger turbidity values. The Linke factor, T_{LK}, is related to the normal beam irradiance (B_n) which is measured through pyrheliometers or estimated by Eq. (1) and is given by the following equation [13,34,38]:

$$T_{LK} = \ln(I_0 * \varepsilon / B_n) * (9.4 + 0.9 * m) / m \quad (3)$$

In which $I_0 * \varepsilon$ is the solar constant corrected by the eccentricity factor due to the variation in the Sun-Earth distance, $I_0 = 1367$ W m^{-2} and $\varepsilon = (R_0 / R)^2$ where R and R_0 denote the instantaneous and mean Sun-Earth distance, respectively. The expressions of $\delta_{RK}(m)$ and $\delta_{Ra}(m)$ are given by the following equations as a function of the optical air mass (m):

$$1/\delta_{Ra} = 6.6296 + 1.7513m - 0.1202m^2 + 0.0065m^3 - 0.00013m^4 \quad (4)$$

$$1/\delta_{RK} = 9.4 + 0.9m \quad (5)$$

$$m = \left[\sin\alpha_s + 0.15 * (3.885 + \alpha_s)^{-1.253}\right]^{-1} \quad (6)$$

Where α_s is the solar elevation angle in degrees which is the compliment angle of solar zenith angle (θ_z).

Once, the hourly values of T_L are obtained, mean daily values are calculated by averaging the hourly ones through the day. In the analysis of T_L, as stated earlier, those hours in which normal beam irradiance is less than 200 W m^{-2} or the clearness index (k_t) < 0.65, or the relative sunshine duration (σ)< 0.9 have been ignored. The time series plots of the hourly T_L values of both stations are shown in Figure 2. The graphs of the stations show a similar pattern. Higher values are observed during the summer months and lower values during the winter months. Higher hourly values range between 6.0 and 9.0 in spring and summer months. Low atmospheric turbidity is noticed during days which are characterized by T_L values in the range of 2.0 and 5.0. The time series plots of the mean daily values of T_L are shown in Figure 3. The mean daily values of T_L range mainly between 2.0 and 5.0. Data reveal a common evolution shape with maxima in summer and minima in winter, mainly due to the daily minimum solar zenith angle and day-length (astronomical factors) variation during the year. Large fluctuations in the spring months and November are mainly due to unstable meteorological conditions during the transition from cold to warm weather and vice versa.

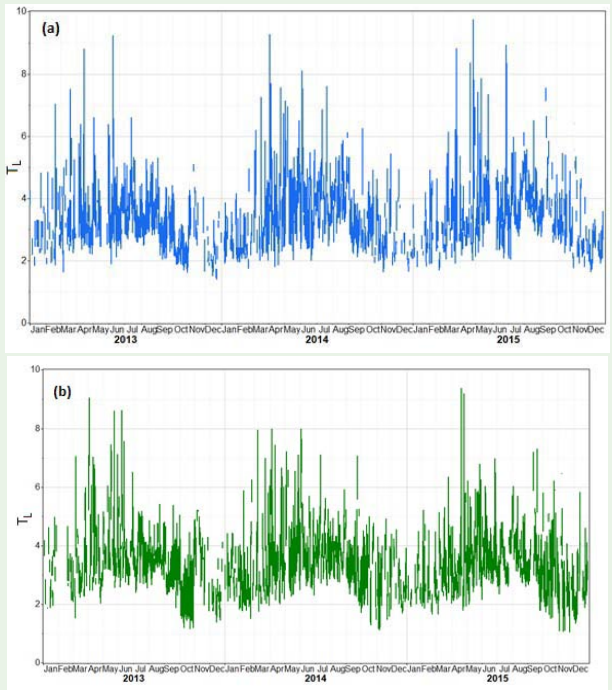

Figure 2: Time series plots of hourly T_L values at a) Athalassa and b) Larnaca.

The calculation method of the Linke Turbidity Factor was extended by estimating it from the global hourly horizontal irradiance, which is a quantity measurable by means of a pyranometer. For this purpose hourly global solar irradiance data for nine stations have been used. The covering period of measurements is about 10 years. The site parameters of the nine stations are listed in Table 1b including the period of records of each station. In this case, the hourly diffuse irradiance is estimated from the correlation of the fraction of diffuse to global irradiance (k_d) through the hourly clearness index (k_t), based on Jacovides et al. [22] correlation:

$$k_d = 0.987$$
$$k_d = 0.94 + 0.937 * k_t - 5.01 * k_t^2 + 3.32 * k_t^3$$
$$k_d = 0.177$$

for $k_t \le 0.1$; $0.1 < k_t \le 0.8$; $k_t > 0.8$ (7)

Then, the diffuse (D) and the direct horizontal irradiances (B) are estimated from the following equations:

$$D = k_d * G \quad (8) \qquad \text{and} \qquad B = G - D \quad (9)$$

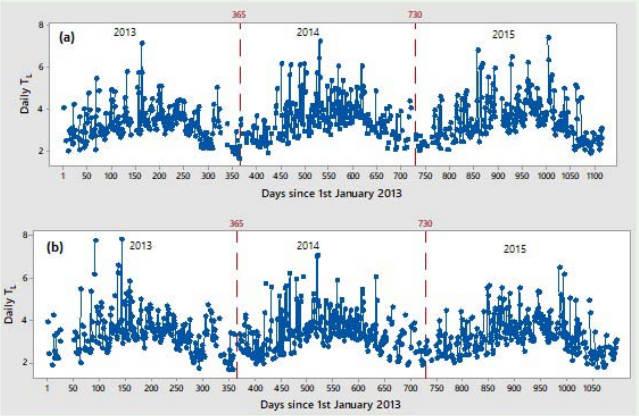

Figure 3: Time series plots of mean daily T_L values at a) Athalassa and b) Larnaca.

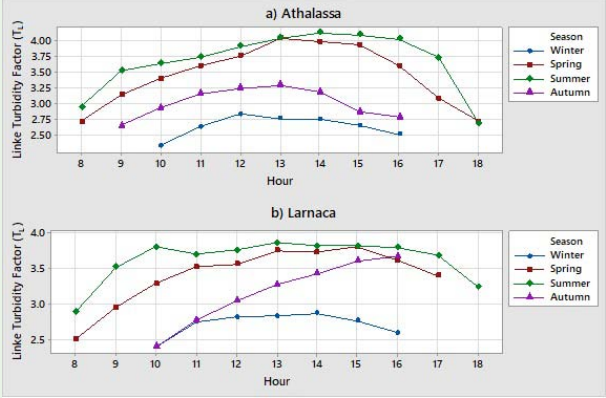

Figure 4: Daily variation of averaged T_L in the different seasons at a) Athalassa and b) Larnaca.

Dividing the direct hourly irradiance (B) by the sine of solar elevation (a_s) (calculated at the centre of the hour), direct hourly normal irradiance (B_n) is obtained, that is, the incident hourly irradiance on a plane perpendicular to the Sun's rays:

$$B_n = B / \sin(a_s) \quad (10)$$

The criteria for the selection of the clear days are those which are referred in section 2.2 by of measurements and quality control processes. Then, the Linke Turbidity Factor (T_{Lk}) is estimated from Eq. (3) as described earlier. The method was also tested for Athalassa and Larnaca using only global solar radiation measurements.

Results and Discussion

Diurnal variation of T_L

A diurnal cycle in the different seasons of Linke turbidity factor is observed at both stations (Figure 4). Athalassa shows slightly higher values than Larnaca. It is characterized by a similar evolution for all the seasons. T_L is increased from morning to afternoon. Maximum values are observed in the summer season and minimum ones are recorded in winter. Slightly lower values than the summer ones are observed in spring. Similar results were obtained by [11-12, 34, 36, 40] in different places of Mediterranean region. The higher diurnal variation is observed in spring and summer at both stations. Mean hourly T_L range mainly between 2.7 and 4.1 in the summer season at Athalassa, while at Larnaca the upper value is slightly lower (3.85). The increase of T_L from morning to afternoon can be attributed to the fact that higher traffic activities are observed during the day at both stations. Details on the effect of temperature, moisture and wind speed and direction on the spatio-temporal variation of turbidity are given in section of turbidity and meteorological parameters.

Monthly variation

Table 4 shows the statistical estimators of the Linke turbidity factor (T_L) for each month of the year including their annual statistics for both stations. The statistical parameters presented in the Table are: number of Data (*N*), Arithmetic Mean (*Mean*), Standard Deviation (*StDev*), Coefficient Of Variation (*CV* in %), Minimum (*Min*), first quartile (*Q1*), *median*, third quartile (*Q3*) and Maximum (*Max*). It can be observed that both stations show similar statistics.

The mean values of T_L range between 2.40 and 3.88 at Athalassa, while at Larnaca they range between 2.52 and 3.85. These values indicate the presence of a clear atmosphere at both stations and both sites are characterized as pure-rural sites. Generally, the monthly mean values of T_L are lower than those obtained by Elshazly [40] in Qena (Egypt), by Djafter and Iirbah [13] in Ghardaïa city (Algeria) and by Ellouz et al. [36] in Northern Tunisia. However, the monthly mean hourly values are comparable to the values obtained by Trabelsi and Masmoudi [12] in Kerkennahisland in Tunisia. The highest mean hourly values occur in May and the lowest in December at both stations. Similar values were obtained by Jacovides et al. [8] at Athalassa station using data covering the period 1985-1993 which shows that the environment in Cyprus is steady in the last 30 years. The

Table 4: Statistical estimators of hourly values of the Linke turbidity factor (T_L) for each month of the year and their annual statistics for both stations.

T_L	a) Athalassa									b) Larnaca								
Month	N	Mean	StDev	CV (%)	Min	Q1	Median	Q3	Max	N	Mean	StDev	CV (%)	Min	Q1	Median	Q3	Max
1	222	2.79	0.63	22.4	1.82	2.34	2.6	3.17	5.42	237	2.92	0.69	23.8	1.84	2.34	2.79	3.37	4.97
2	309	2.73	0.82	30.1	1.72	2.22	2.45	2.99	7.04	261	2.77	0.84	30.4	1.53	2.18	2.53	3.1	6.26
3	416	3.22	1.05	32.5	1.66	2.54	2.89	3.63	8.83	442	3.13	1.08	34.6	1.55	2.42	2.8	3.48	8.71
4	526	3.56	1.24	35	1.83	2.78	3.16	3.9	9.76	558	3.51	1.23	35.1	1.81	2.7	3.16	3.9	9.37
5	490	3.88	1.03	26.5	2.05	3.14	3.74	4.43	8.21	611	3.85	1.06	27.5	2	3.14	3.62	4.35	9.12
6	694	3.7	1.01	27.3	1.91	3.09	3.51	4.06	9.23	784	3.75	0.89	23.8	2.18	3.17	3.54	4.07	8.62
7	808	3.74	0.72	19.4	2.06	3.23	3.59	4.15	7.61	864	3.66	0.64	17.6	2.25	3.2	3.58	4.08	7.12
8	695	3.87	0.63	16.3	2.38	3.42	3.8	4.23	6.51	727	3.74	0.6	16	2.53	3.34	3.65	4.02	6.04
9	503	3.43	0.85	24.9	2.05	2.91	3.22	3.74	7.55	568	3.36	0.84	25.1	1.8	2.82	3.17	3.68	7.31
10	445	2.85	0.69	24.1	1.6	2.32	2.72	3.2	5.46	497	2.85	0.89	31.3	1.17	2.24	2.72	3.4	6.46
11	259	2.84	0.84	29.7	1.65	2.22	2.61	3.15	6.43	302	2.88	1.01	35.1	1.07	2.16	2.71	3.54	6.45
12	258	2.4	0.61	25.3	1.41	2	2.26	2.62	5.91	296	2.52	0.77	30.4	1.35	2.02	2.38	2.86	6.92
Year	5625	3.41	0.99	28.9	1.41	2.73	3.28	3.92	9.76	6147	3.4	0.98	28.8	1.07	2.75	3.29	3.89	9.37

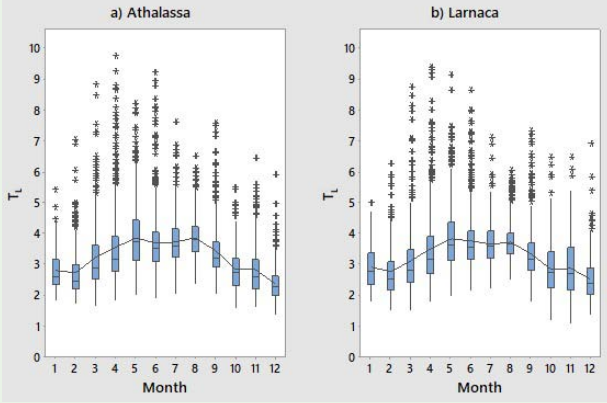

Figure 5: Boxplots of the hourly T_L for each month of the year at both stations.

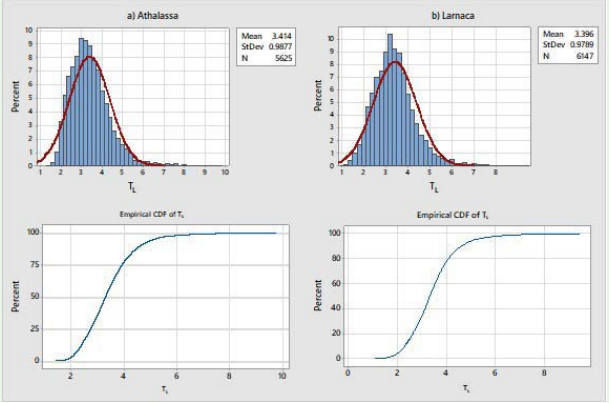

Figure 6: Frequency distributions and cumulative frequency distributions of hourly T_L for the period 2013-2015 for a) Athalassa and b) Larnaca.

annual variation of the turbidity in Cyprus is related to the prevailing weather conditions throughout the year. During spring dust from the Arabian and African deserts is transferred over the greater area of Cyprus. This results in increasing levels of atmospheric turbidity during the same period [41]. The abrupt reduction of turbidity in October is due to the rains observed at the end of this month after a long period of dryness (summer months).

The median values are generally lower than the means. The standard deviation of the measurements at both stations varies between 0.60 and 1.24. The higher values of the standard deviation are recorded in the spring season. As a result the coefficients of variation in the spring are higher than the other months and range between 26.5 and 35.0% at Athalassa. Slightly higher values are observed at Larnaca (27.5 and 35.1%). The minimum values of standard deviation are observed in the summer months at both stations, indicating more stable conditions during this season. Maximum values of hourly T_L up to 9 are obtained during the spring and summer seasons. The variability of the hourly T_L for each month of the year is also shown in Figure 5 for both stations. The boxplots show a number of outliers at the upper part of the boxes in each month of the year. Higher variability is observed in the spring months (March-May).

Table 5 presents the seasonal variation of Linke turbidity factor for the morning and afternoon hours for both stations in terms of mean and standard deviation values. During the winter season, turbidity is minimum for both stations with almost similar values in the morning and afternoon hours.The turbidity during the winter season is lower than the other seasons, since this is the main rainy season of the year. As one advances from winter to the rest of the year the turbidity increases from morning towards the afternoon hours.

Table 5: Seasonal variation of Linke turbidity factor for morning and afternoon hours at Athalassa and Larnaca.

		Athalassa		Larnaca	
Season	**Day Time**	**Mean**	**St Dev**	**Mean**	**St Dev**
Winter	Morning	2.638	0.708	2.670	0.767
	Afternoon	2.634	0.746	2.771	0.806
Spring	Morning	3.522	1.137	3.320	1.096
	Afternoon	3.669	1.161	3.734	1.191
Summer	Morning	3.648	0.800	3.654	0.755
	Afternoon	3.989	0.761	3.765	0.697
Autumn	Morning	3.076	0.873	2.686	0.852
	Afternoon	3.135	0.733	3.470	0.838

Frequency distribution of hourly T_L

The frequency distribution of Linke turbidity has been computed from hourly values of turbidity and the results are presented in Figure 6. It is seen that the frequency distributions over the whole period for both stations are asymmetric. The peak frequency at both stations is about 10% representing the class interval 2.5-3.5. The curve on the graph is the normal probability curve. The cumulative frequency distributions (CDF) of T_L are shown below the Probability Density Function (PDF) graph of each station. It can be noted that 37% of T_L values are less than 3, 50% are between 3 to 5 and only 13% are greater than 5. Almost similar values were observed at Qena (Egypt) [40] and at Ghardaïa city (Algeria) [13].

The cumulative frequency distributions for each season and station are shown in Figure 7. The similarities between the two

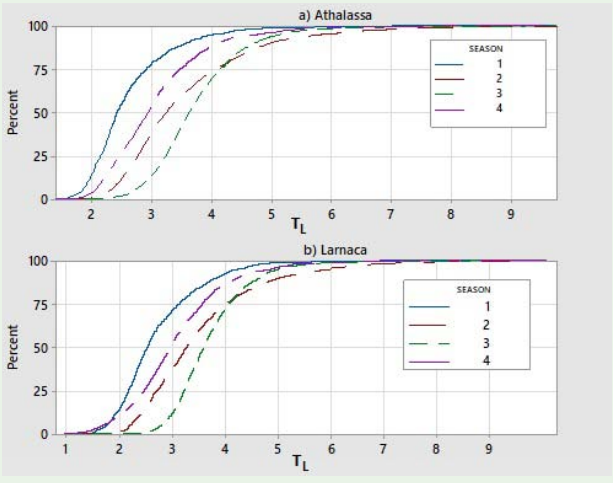

Figure 7: Cumulative Frequency Distribution (CDF) of T_L values for each season at a) Athalassa and b) Larnaca. (Season 1: Winter), (Season 2: Spring) (Season 3: Summer) (Season 4: Autumn).

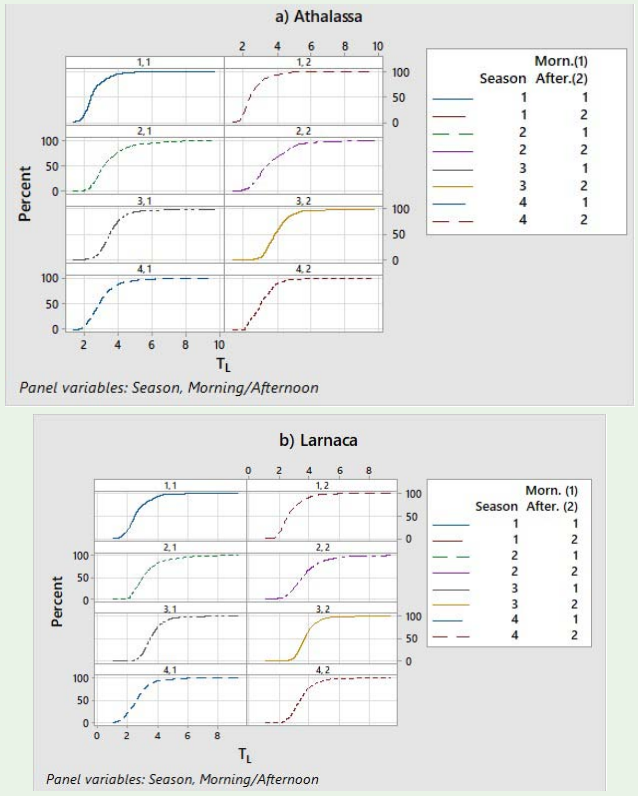

Figure 8: Cumulative frequency distribution (CDF) of T_L values for each season and morning or afternoon hours at a) Athalassa and b) Larnaca.

Table 6: Probabilities for the T_L values less than 4 or greater than or equal to 4 for the combination of the seasons (1 to 4) and the morning or afternoon hours (1 to 2), (1: Winter season 2: Spring season 3: Summer season 4: Autumn season), (Morning Hours:1, Afternoon Hours:2)

Season / Time of Day	Athalassa		Larnaca	
	$T_L < 4$	$T_L \geq 4$	$T_L < 4$	$T_L \geq 4$
	Probabilities (%)			
1/1	95	5	93	7
1/2	94	6	92	8
2/1	78	22	81	19
2/2	68	32	66	34
3/1	74	26	78	22
3/2	57	43	67	33
4/1	87	13	93	7
4/2	91	9	79	21

stations are evident. In winter, (Season 1: December-February), at Athalassa, T_L is less than 4 in 94%, i.e., it is exceeding this level in 6%. In spring, (Season 2: March-May), T_L is less than 4 in 74%, in summer, (season 3: June-August), in 69% and in autumn, (season 4: September-November) in 87%.

The cumulative frequency distributions for each season with respect to the morning and afternoon hours for each station are shown in Figure 8. Table 6 presents the probabilities for the cases of T_L values less to be than 4 or greater than or equal to 4 for the combination of the season and the morning or afternoon hours. Generally, the probabilities of exceeding the value of T_L=4 are higher in the afternoon hours in all the seasons at both stations, with the

Table 7: Statistics of T_L values for different vapour pressure (hPa) ranges at both stations.

Bin Endpoints		Athalassa						Larnaca					
Vapour pressure (hPa)		Linke Turbidity Factor (T_L)						Linke Turbidity Factor (T_L)					
Lower	Upper	Occurr.	Mean	Median	Min	Max	Std. Dev.	Occurr.	Mean	Median	Min	Max	Std. Dev.
2	4	25	2.284	2.247	1.818	2.918	0.235	8	2.182	2.096	1.964	2.617	0.251
4	6	207	2.497	2.294	1.412	7.521	0.788	119	2.166	2.048	1.336	3.857	0.502
6	8	425	2.914	2.634	1.603	9.758	1.091	225	2.405	2.377	1.065	7.058	0.763
8	10	776	3.02	2.878	1.467	8.827	0.903	353	2.728	2.542	1.099	6.99	0.856
10	12	1014	3.188	3.023	1.646	9.274	0.947	697	2.9	2.659	1.131	7.434	0.883
12	14	825	3.524	3.318	1.769	8.362	0.98	659	3.205	3.039	1.115	9.187	1.034
14	16	665	3.652	3.551	1.911	8.352	0.85	622	3.401	3.214	1.496	9.123	0.996
16	18	569	3.594	3.517	2.014	9.233	0.837	520	3.571	3.384	1.651	9.372	1.014
18	20	428	3.738	3.676	2.06	8.763	0.794	607	3.609	3.443	1.832	7.989	0.976
20	22	277	3.958	3.955	2.194	6.601	0.751	618	3.578	3.391	1.802	8.621	0.847
22	24	193	4.181	4.123	2.923	6.859	0.729	534	3.634	3.472	2.098	7.972	0.818
24	26	80	4.419	4.272	3.096	6.616	0.769	544	3.764	3.667	2.324	7.199	0.672
26	28	29	4.464	4.414	3.449	6.701	0.745	422	3.977	3.887	2.534	6.955	0.692
28	30	4	4.512	4.704	3.989	4.807	0.365	261	4.001	3.904	2.579	7.115	0.689
30	32							62	4.029	3.904	2.711	6.878	0.732
32	34							5	4.007	3.177	3.157	6.452	1.423

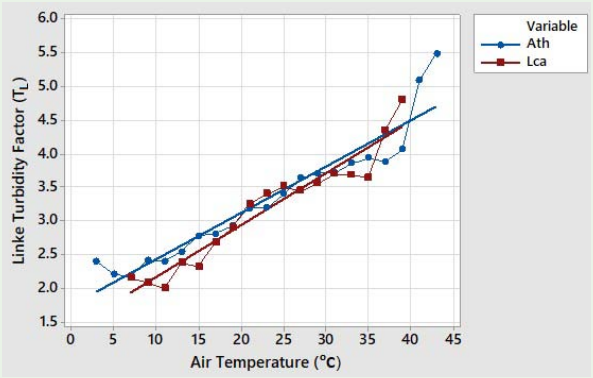

Figure 9: Variation of mean Linke Turbidity Factor (T_L) with air temperature (°C) at both stations.

exception of the autumn season at Athalassa. The differences between the morning and afternoon hours are higher in the spring and summer season.

Turbidity and meteorological parameters

The short-term variation of atmospheric turbidity depends on local weather conditions (temperature, vapour pressure, wind speed and wind direction) and its long-term one on the climate of the area. Figure 9 shows the dependence of T_L with respect to air temperature values at both stations. The Linke turbidity factor is increased linearly with air temperature at both stations. The slopes of the regression lines of the two stations are almost similar. This figure also shows that the maximum of T_L is recorded in higher temperature because of the increase of the vertical convection which is enchased by water vapour in the atmosphere, especially in a summer season. The Linke turbidity factor is also increased with increasing the vapour pressure at both stations (Table 7). Similar results were obtained by Trabelsi and Masmoudi [12] at Kerkennahisland in Tunisia.

The prevailing winds, which may transport moisture or aerosol particles from distant sources, play a major role in the spatio-temporal variation of turbidity. Wind speed also plays a significant role in the transport of moisture or aerosol particles.

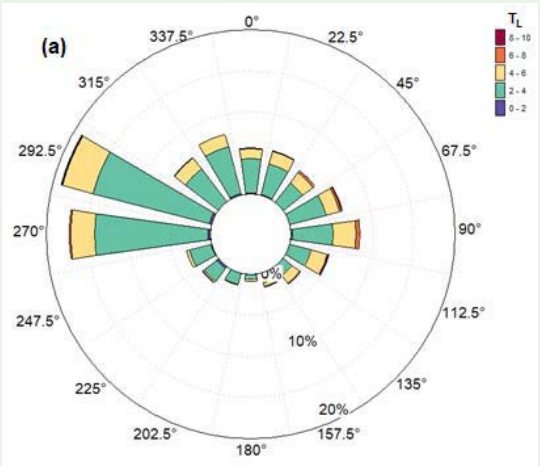

Figure 10a: Wind rose of hourly T_L at Athalassa.

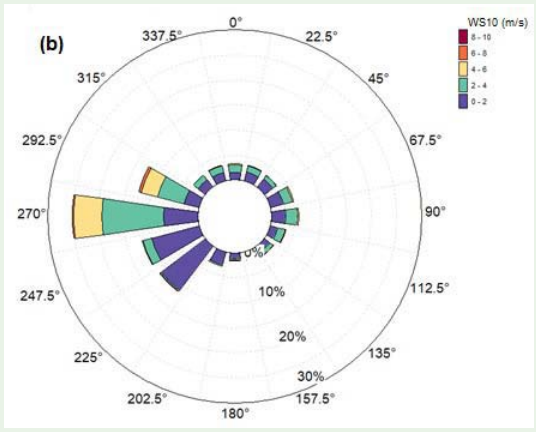

Figure 10b: Wind rose of hourly wind speed at the height of 10 m at Athalassa.

At Athalassa, the prevailing wind direction during the day is Westerlies and most of the traffic pollutants are transferred from the Nicosia city towards the monitoring station at Athalassa which is located in the eastern part of the city. Hazy conditions are associated mainly with Easterlies winds (Figures 10a and 10b).

In the case of Larnaca the higher values of T_L in the afternoons are associated with the sea breeze circulation which favours a load of water vapour in the local atmosphere and the increase of air traffic during the day at the airport which is located next to the monitoring station. During the night the prevailing wind directions at Larnaca are North-Westerlies (land breezes) (Figures 10c and 10d). Figure 10d shows that land breezes during the night may transfer aerosol particles from the land surfaces towards the monitoring station, therefore, increasing the pollutants during the day. These aerosol particles in combination to the sea breeze circulation in the afternoon favour a load of water vapour in the local atmosphere and therefore the turbidity is higher in the South-westerlies direction (Figure 10c).

The influence of wind speed on the variation of turbidity is shown in Table 8. The turbidity factor was estimated for different intervals of 1 m s^{-1}. Higher wind speeds are recorded at Larnaca (Tables 3 & 8).

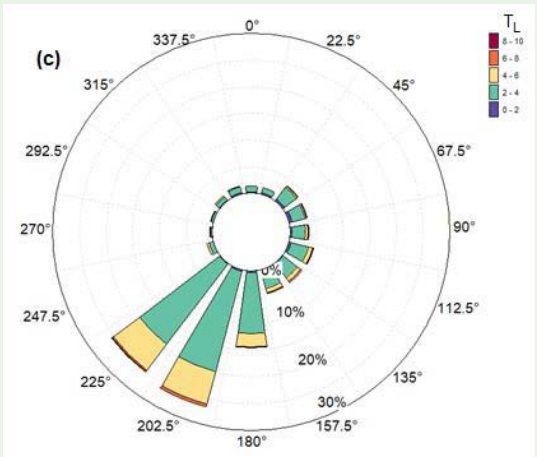

Figure 10c: Wind rose of hourly T_L at Larnaca.

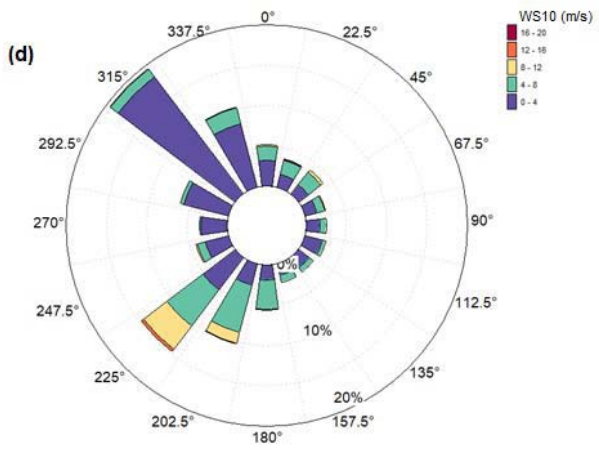

Figure 10d: Wind rose of hourly wind speed at the height of 10 m at Larnaca.

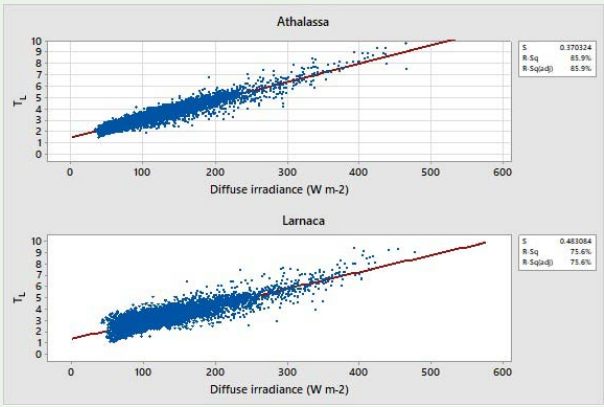

Figure 11: Linear relationship between T_L and hourly diffuse irradiance at both stations.

At Athalassa, T_L remains almost constant up to 5 m s^{-1} and then it is slightly increased with increasing wind speed up to 7m s^{-1}. However, at higher wind speeds T_L decreases. On the other hand, T_L at Larnaca is increased with the increase of mean hourly wind speed. Similar results were obtained by Trabelsi and Masmoudi [12] at Kerkennahisland in Tunisia and Ellouz et al. [36] in Northern Tunisia.

The relationship between T_L and hourly diffuse irradiance (D) is shown in Figure 11 for both stations. A linear line was fitted in both cases. The slopes of the fitted lines are almost identical. Most of the values of diffuse irradiance are concentrated in the range between 50 and 300 W m^{-2}. In equation form these are given by:

$$T_{L-Ath} = 1.429 + 0.016 * D \qquad R^2 = 0.859 \qquad (11)$$

$$T_{L-Lca} = 1.351 + 0.015 * D \qquad R^2 = 0.756 \qquad (12)$$

Comparison of T_L values for different sites in Cyprus

As indicated earlier, the Linke Turbidity Factor (T_L) was estimated for nine locations in Cyprus, representing different climatic conditions by using hourly global solar irradiance data covering mainly the period 2000-2010 (Table 1b). The two methods were compared using the datasets of the two stations (Athalassa and Larnaca) for the period 2013-2015. The results showed that the second method (only hourly data of global irradiance) can be also effectively used to estimate the Linke Turbidity Factor. The following

Table 8: Statistics of T_L values for different mean hourly wind speed (m s^{-1}) ranges at both stations.

Bin Endpoints		Athalassa						Larnaca					
Wind Speed 10 m (m s^{-1})		Linke Turbidity Factor (T_L)						Linke Turbidity Factor (T_L)					
Lower	Upper	Occur.	Mean	Median	Min	Max	Std. Dev.	Occur.	Mean	Median	Min	Max	Std. Dev.
0	1	269	3.013	2.818	1.646	6.933	0.871	9	3.734	3.522	2.341	5.901	1.231
1	2	1293	3.451	3.347	1.661	9.758	0.994	121	3.127	3.047	1.065	7.562	1.093
2	3	1007	3.571	3.425	1.77	8.936	1.027	462	3.058	2.877	1.076	9.123	1.105
3	4	502	3.5	3.377	1.718	8.827	1.075	796	3.238	3.027	1.175	9.053	1.103
4	5	310	3.502	3.394	1.84	7.944	1.083	1126	3.328	3.225	1.131	9.187	0.956
5	6	161	3.659	3.572	1.677	8.362	1.12	1089	3.402	3.292	1.346	8.714	0.923
6	7	37	3.645	3.568	2.275	6.733	1.043	859	3.421	3.343	1.115	7.434	0.892
7	8	16	3.158	2.994	2.302	4.602	0.627	605	3.544	3.481	1.314	7.965	0.902
8	9	3	2.961	2.961	2.669	3.253	0.292	477	3.612	3.529	1.541	7.561	0.91
9	10	4	2.835	2.961	2.366	3.069	0.317	344	3.626	3.529	1.099	9.372	0.904
10	11							189	3.65	3.454	1.399	7.989	1.022
11	12							107	3.776	3.665	1.96	6.338	0.888
12	13							57	3.597	3.356	2.155	5.598	0.861
13	14							10	3.841	3.716	2.253	5.394	1.131
14	15							5	4.794	5.061	3.614	5.472	0.724
15	16							1	4.444	4.444	4.444	4.444	0

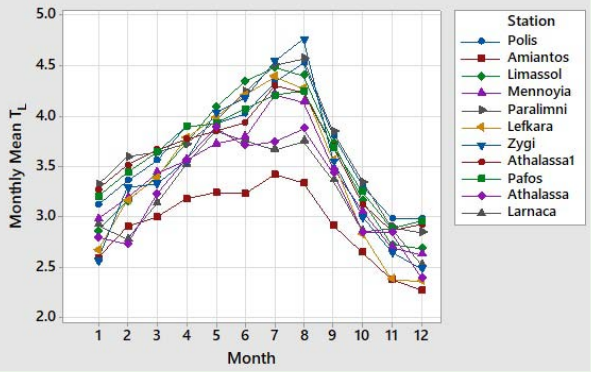

Figure 12: Monthly mean values of T_L for different locations in Cyprus for the period 2000-2010 and for Athalassa and Larnaca with measurements taken during the period 2013-2015. Athalassa1 is the station with measurements in the period 2000-2010.

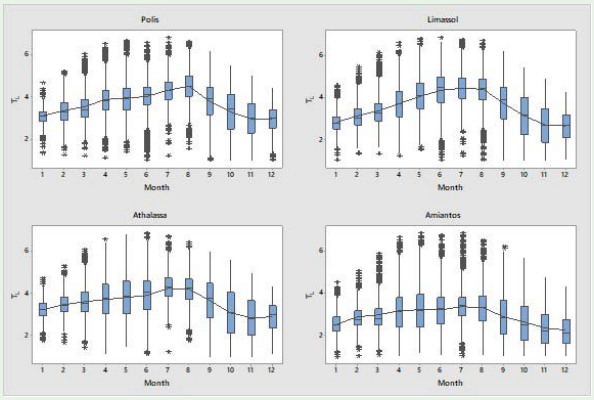

Figure 14: Monthly boxplots of hourly T_L for two coastal stations (Polis and Limassol) one inland plain station (Athalassa) and one station at high altitude (Amiantos).

equations have been obtained from the relationship of the estimated T_L values using the two methods for the two stations:

$$T_{L\_Ath\_2} = 1.012 * T_{L\_Ath\_1} \quad R^2 = 0.950 \qquad (13)$$

$$T_{L\_Lca\_2} = 0.996 * T_{L\_Lca\_1} \quad R^2 = 0.970 \qquad (14)$$

where, method 2 is the method of estimating T_L values from the hourly global irradiance data and method 1 is the method of estimating T_L values from hourly global and diffuse irradiance data. The slopes of the lines of the equations and the coefficient of determinations of both stations are close to one.

As indicated earlier the second method was implemented for nine locations in Cyprus. The results of this calculation are shown in Figure 12. The graph has additionally the monthly mean values of T_L of Athalassa and Larnaca with the latest period of measurements (2013-2015). It is clear from the graph that the station of Amiantos has the lowest values of T_L, since this station is located in the mountainous area with a clearer atmosphere than the other sites. The pattern of T_L throughout the year is similar to all the stations. The differences between the stations are relatively small with the highest values of T_L occurring in the southern coastal areas. The values of T_L during the summer season of the latest period of measurements are generally lower than those obtained during the period of 2000-2010.

The differences of T_L between the high altitude station (Amiantos) and the rest of the stations are illustrated in Figure 13, which shows the cumulative density function of T_L of each station. The probability of having $T_L < 4$ at Amiantos is about 83%, while for the rest of the stations is around 60%. The variability of the hourly T_L values is shown in the graph with the boxplots for four stations (two coastal stations: Polis and Limassol, one inland plain station (Athalassa) and one at high altitude station (Amiantos) in Figure 14. The curve which connects the boxplots of each month is the monthly mean of the hourly T_L values. The characteristic of the boxplots is the absence of outliers (asterisks) during the period September-December for all the stations. The similarities of the coastal and inland plain stations are evident.

There is a linear relationship between the hourly Linke turbidity factors of the above stations. Most of the coefficients of determination (R^2) for these linear relationships range between 0.6 and 0.7. However, R^2 is equal to 0.8 for the relationship between T_L of Mennoyia and Zygi, (Figure 15) since the two stations are very close (see Figure 1).

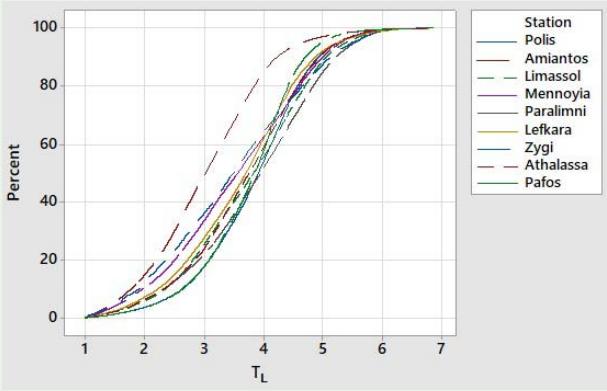

Figure 13: Cumulative Density Function (CDF) of hourly T_L for the selected stations.

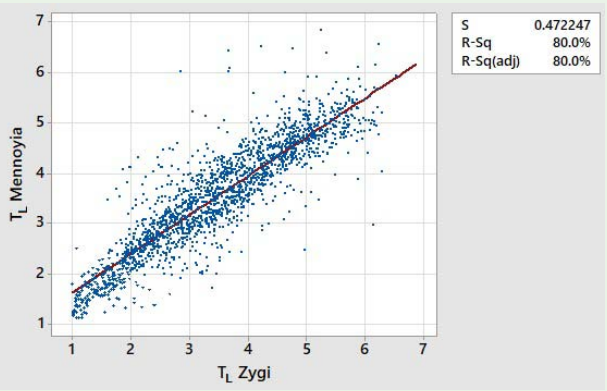

Figure 15: Linear relationship of the hourly Linke turbidity factors between Mennoyia and Zygi. $T_{L\_Men} = 0.836 + 0.776 * T_{L\_Zyg}$

Table 9: Statistical estimators of the mean daily values of Linke turbidity factor at both stations.

	Athalassa									Larnaca								
Month	**N**	**Mean**	**StDev**	**CV (%)**	**Min**	**Q1**	**Median**	**Q3**	**Max**	**N**	**Mean**	**StDev**	**CV (%)**	**Min**	**Q1**	**Median**	**Q3**	**Max**
1	40	2.76	0.51	18.55	1.98	2.38	2.66	3.01	4.16	43	2.95	0.64	21.6	1.89	2.39	2.86	3.38	4.26
2	55	2.81	0.69	24.71	1.87	2.28	2.62	3.32	4.74	45	2.78	0.72	26.04	1.91	2.34	2.58	3.12	5.75
3	65	3.33	0.87	26.11	2.01	2.72	3	3.95	6.12	65	3.14	0.86	27.39	1.98	2.52	2.85	3.74	5.59
4	72	3.63	1.02	28.03	2.38	2.89	3.27	4.06	6.74	74	3.63	1.12	30.8	2.27	2.81	3.27	4.24	7.79
5	67	3.9	0.84	21.6	2.7	3.31	3.66	4.42	6.12	81	3.95	0.94	23.8	2.43	3.31	3.7	4.44	7.86
6	81	3.81	0.98	25.58	2.74	3.2	3.51	3.98	7.19	90	3.84	0.85	22.17	2.77	3.25	3.61	4.13	7.11
7	92	3.83	0.69	18.08	2.78	3.29	3.67	4.27	6.18	92	3.71	0.59	15.83	2.54	3.22	3.64	4.08	5.89
8	92	3.95	0.57	14.47	3	3.54	3.9	4.22	6.01	93	3.78	0.54	14.41	2.94	3.36	3.69	4.07	5.47
9	74	3.51	0.85	24.17	2.65	2.99	3.28	3.7	7.37	83	3.4	0.78	22.87	2.52	2.93	3.2	3.6	6.51
10	72	2.92	0.62	21.19	2.06	2.39	2.84	3.36	4.92	74	2.91	0.69	23.8	1.74	2.38	2.89	3.2	5.04
11	49	2.9	0.83	28.72	2.01	2.31	2.58	3.3	5.12	51	2.97	0.84	28.18	1.75	2.27	2.78	3.5	4.94
12	47	2.43	0.58	23.7	1.61	2.01	2.27	2.67	4.36	52	2.49	0.54	21.79	1.66	2.01	2.44	2.76	3.89
Year	806	3.42	0.91	26.71	1.61	2.8	3.3	3.9	7.37	843	3.4	0.9	26.38	1.66	2.78	3.29	3.86	7.86

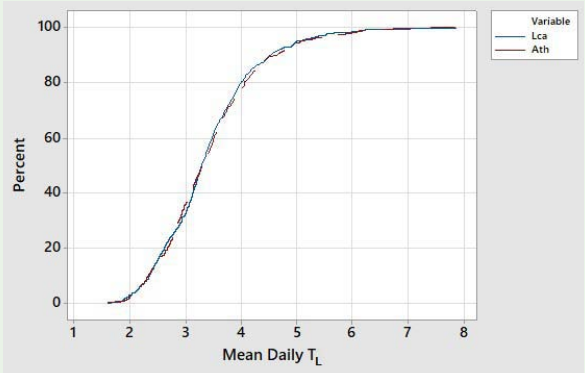

Figure 16: Cumulative frequency distribution of mean daily T_L values at the two stations.

Analysis of mean daily values of T_L

Mean daily Linke turbidity values were obtained by averaging the hourly values. Days with more than half number of hours of the day time interval were considered in the analysis. Figure 3 shows the time series plots of mean daily T_L values, while Table 9 presents the statistical estimators of the mean daily values of Linke turbidity factor at both stations. The monthly mean daily values of T_L range mainly between 2.5 and 4.0 at both stations, while their standard deviation range mainly between 0.5 and 1.1 with the highest occurring in spring months. The increases of mean daily T_L values from winter to summer is generally associated with an increase of temperature, vapour pressure, wind speed and decrease in relative humidity (see Table 3). This change in these weather elements leads to an increase in the content of dust and water vapour in the atmosphere and consequently higher values of T_L. The median values are generally slightly lower than the mean values.

Figure 16 shows the cumulative frequency curves of the mean daily T_L values for both stations. The similarities of the distribution of the two stations are evident. In 80% of the cases, both stations, have mean daily T_L values lower than 4.0.

Conclusion

The Linke turbidity factor (T_L) has been derived from hourly global and diffuse irradiance measurements at two sites in Cyprus, one inland location (Athalassa) and one coastal location (Larnaca) representing different climate regimes using three years of measurements (2013-2015). The method of calculating the T_L values has been extended by calculating the diffuse irradiance from global irradiance measurements, based on known relationships between the hourly fraction of diffuse to global irradiance and the clearness index values. The method was firstly tested on the data of Athalassa and Larnaca for the period of 2013-2015 with satisfactory results and then it was implemented to nine stations distributed in various locations over the island which are equipped with pyranometers and measure only global irradiance, during the period 2000-2010.

The daily and monthly variation of atmospheric turbidity has been studied. It was found that atmospheric turbidity decreases during the winter season (rainy season) and increases during the summer season. Athalassa shows slightly higher values than Larnaca. The higher diurnal variation is observed in spring and summer at both stations. Mean hourly T_L range mainly between 2.7 and 4.1 in the summer season at Athalassa, while at Larnaca the upper value is slightly lower (3.85). The annual mean values of T_L are 3.40 at both stations. T_L is increased from morning to afternoon. The increase of T_L from morning to afternoon can be attributed to the fact that higher traffic activities are observed during the day at both stations. The presented here results are comparable to those recorded in different places in Mediterranean region.

The mean values and frequency of occurrence of T_L have been used to characterize the atmospheric turbidity over Cyprus. The peak frequency at both stations is about 10% representing the class interval 2.5-3.5. The Cumulative Frequency Distributions (CDF) of T_L shows that about 37% of T_L values are less than 3, 50% are between 3 to 5 and

only 13% are greater than 5. This indicates that the skies on cloudless days are clean and clear.

The short-term variation of atmospheric turbidity depends on local weather conditions (temperature, vapour pressure, wind speed and wind direction) and its long-term one on the climate of the area. It was found that the Linke turbidity factor is increased linearly with air temperature at both stations. T_L is also increased with increasing the vapour pressure at both stations.

The prevailing winds, which may transport moisture or aerosol particles from distant sources, play a major role in the spatio-temporal variation of turbidity. Wind speed also plays a significant role in the transport of moisture or aerosol particles. At Athalassa, the prevailing wind direction during the day is Westerlies and most of the traffic pollutants are transferred from the Nicosia city towards the monitoring station at Athalassa which is located in the eastern part of the city. Hazy conditions are associated mainly with Easterlies winds. In the case of Larnaca the higher values of T_L in the afternoons are associated with the sea breeze circulation which favours a load of water vapour in the local atmosphere and the increase of air traffic during the day at the airport which is located next to the monitoring station. During the night the prevailing wind directions at Larnaca are North-Westerlies (land breezes) that may transfer aerosol particles from the land surfaces towards the monitoring station, therefore increasing the pollutants during the day.

The diffuse irradiance is increased with the increase of atmospheric turbidity. Linear relationships were established between them.

Comparing the T_L values of different locations over the island, it was found that the high altitude station (Amiantos) has the lowest values, since this station has clearer atmosphere than the other sites. The pattern of T_L throughout the year is similar to all stations. The differences between the stations are relatively small with the highest values of T_L occurring in the southern coastal areas. The values of T_L during the summer season of the latest period of measurements (2013-2015) are generally lower than those obtained during the period of 2000-2010.

Nomenclature

B	Horizontal beam irradiance [Wm^{-2}]
B_n	Normalbeam irradiance [Wm^{-2}]
CDF	Cumulative Probability Density Function
CV	Coefficient of Variation [%]
D	Diffuse solar irradiance [Wm^{-2}]
e	Vapour pressure [hPa]
G	Global solar irradiance [Wm^{-2}]
G_0	Extraterrestrial irradiance [Wm^{-2}]
I_0	Solar constant [1367 Wm^{-2}]
k_d	Hourly fraction of diffuse to global irradiance ($k_d = D/G$)
k_t	Hourly clearness index ($k_t = G/G_0$)
m	Optical air mass
Max	Maximum
Min	Minimum
N	Nonmissing observations
N^*	Missing observations
n	Julian day number (1..365)
PDF	Probability density function
$Q1$	First Quartile
$Q3$	Third Quartile
R	Instantaneous Sun-Earth distance
R_0	Mean Sun-Earth distance
$StDev$	Standard deviation
T_a	Air temperature [^{0}C]
T_L	Linke turbidity factor
T_{LK}	Kasten turbidity factor
T_{Lm}	Long-term monthly average T_L value
W_{d10m}	Wind direction at 10 m height [degrees]
W_{s10m}	Wind speed at 10 m height [m s^{-1}]

Greek:

a_s	Solar elevation angle [degrees]
β	Ångström turbidity coefficient
$\delta_{RK}(m)$	Rayleigh optical thickness given by Kasten
$\delta_{Ra}(m)$	Optical thickness given by Louche et al. and adjusted by Kasten
θ_z	Solar zenith angle (SZA) [degrees]
δ	Solar declination [degrees]
ε	eccentricity correction $\varepsilon = (R_0/R)^2$
σ	relative sunshine duration
φ	Latitude [degrees]

References

1. Bilbao J, Román R, Miguel A. Turbidity coefficients from normal direct solar irradiance in Central Spain. Atmospheric Research. 2014; 143: 73-84.
2. Narain L, Garg S. Estimation of Linke turbidity factors for different regions of India. Int J Environment and Easte Management. 2013; 12: 52-64.
3. Pedrós R, Utrillas MP, Martinez-Lozano JA, Tena F. Values of broadband turbidity coefficients in a Mediterranean coastal site. Solar Energy. 1999; 66: 11-20.
4. Scharmer K. Greif J. The European Solar Radiation Atlas. ESRA Database and exploitation software. 2000; 2.
5. Remund J, Wald L, Lefevre M, Ranchin T, Page J. Worldwide Linke turbidity information. Proceedings of ISES Solar World Congress, 16-19 June, Göteborg, Sweden, CD-ROM published by International Solar Energy Society. 2003.
6. Ellouz F, Masmoud M, Medhioubet K. Study of the atmospheric turbidity over Northern Tunisia. Renewable Energy. 2008; 2: 1-5.

Citation: Pashiardis S, Kalogirou SA and Pelengaris A. Statistical Analysis and Inter-Comparison of Linke Turbidity Factor for Two Sites in Cyprus: Athalassa (Inland Location) and Larnaca (Coastal Location). SM J Biometrics Biostat. 2018; 3(2): 1029.

7. Page JK. Solar Energy R&D in the European Community Series F Solar Radiation data. Prediction of solar radiation on inclined surfaces. D. Reidel Publishing Company. 1986; 3.

8. Jacovides C, Timbios F, Giannourakos G, Pashiardis S, Stefanou L. Recent measurements of broad-band turbidity parameters in the island of Cyprus. Atmospheric Environment. 1996; 30: 3391-3396.

9. Cucumo M, Marinelli V, Oliveti G. Experimental data of the Linke Turbidity factor and estimates of the Ångström turbidity coefficient for two Italian localities. Renewable Energy. 1999; 17: 397-410.

10. Kambezidis H, Fotiadi A, Katsoulis B. Variability of the Linke and Unsworth-Monteith turbidity parameters in Athens, Greece. Meteorol Atmos Phys. 2000; 75, 259-269.

11. Chaâbane M. Analysis of the atmospheric turbidity levels at two Tunisian sites. Atmospheric Research. 2008; 87: 136-146.

12. Trabelsi A, Masmoudi M. An investigation of atmospheric turbidity over Kerkennah island in Tunisia. Atmospheric Research. 2011; 101: 22-30.

13. Djafter D. Irbah A. Estimation of atmospheric turbidity over Ghardaïa city. Atmospheric Research. 2013; 128: 76-84.

14. Louche A, Maurel M, Simonnot G, Peri G, Iqbal M. Determination of Ångström's turbidity coefficient from direct total solar irradiance measurements. Solar Energy. 1987; 38: 89-96.

15. Dogniaux R. Représentations analytiques des composantes du rayonnementlumineuxsolaire. Conditions du ciel serein. Institut Royal de Météorologie de Belgique, Série A. No. 83. 1974.

16. ESRA. European Solar Radiation Atlas published for the Commission of the European Communities by Presses de l' Ecole, Ecole des Mines de Paris, Paris, France. 1999.

17. Dogniaux R, Lemoine M. In Palz (Ed.), Solar Energy R&D in the European Community, Series F. Solar Radiation Data. D. Reidel Publ., Dordrecht, 1983; 2: 94-107.

18. Jacovides C, Kaltsunides N, Hachioannou L, Stefanou L. An assessment of the solar radiation climate of the Cyprus environment. Renewable Energy. 1993; 3: 913-918.

19. Kambezidis H. Typical Meteorological Year for Nicosia. Theory and user guide. 1999.

20. Kalogirou SA. Generation of typical meteorological year (TMY-2) for Nicosia, Cyprus. Renewable Energy. 2003; 28: 2317-2334.

21. Kalogirou S, Pashiardis S. Pashiardi A. Statistical analysis and inter-comparison of the global solar radiation at two sites in Cyprus. Renewable Energy. 2017; 101: 1102-1123.

22. Jacovides CP, Tymvios FS, Assimakopoulos VD, Kaltsounides NA. Comparative study of various correlations in estimating hourly diffuse fraction of solar radiation. Renewable Energy. 2006; 31: 2492-2504.

23. World Meteorological Organization. WMO Guidelines on the quality control of data from the World Radiometric Network. WCDP-3, WMO/TD-No.258, p 30, WMO, Geneva, Switzerland. 1987.

24. Long CN, Dutton EG. 2002. Global Network recommended QC tests. V2.0, BSRN Technical Report.

25. Muneer T. Solar Radiation and Daylight models.2nd Edition. Oxford: Elsevier. 2004.

26. Long CN, Shi Y. An automated quality assessment and control algorithm for surface radiation measurements. The Open Atmospheric Science Journal. 2008; 2: 23-37.

27. Pashiardis S, Kalogirou S. Quality control of solar shortwave and terrestrial longwave radiation for surface radiation measurements at two sites in Cyprus. Renewable Energy. 2016; 96: 1015-1033.

28. Iqbal M. An introduction to solar radiation. Toronto: Academic Press. 1983.

29. Rigollier C, Bauer O, Wald L. On the clear sky model of the 4th European Solar Radiation Atlas with respect to Heliosat method. In: Solar Energy. 2000; 68: 33-48.

30. Mavromatakis F, Franghiadakis Y. Direct and indirect determination of the Linke turbidity coefficient. Solar Energy. 2007; 81: 896-903.

31. Jacovides C. Model comparison for the calculation of Linke's turbidity factor. Inernational Journal of Climatology. 1997; 17: 551-563.

32. Ineichen P, Perez R. A new air mass independent formulation for the Linke turbidity coefficient. Solar Energy. 2002; 73: 151-157.

33. Danny H, Lam J. A study of atmospheric turbidity for Hong Kong. Renewable Energy. 2002; 25: 1-13.

34. Chaâbane M, Masmoudi M, Medhioub K. Determination of Linke turbidity factor from solar radiation measurement in northern Tunesia. Renewable Energy. 2004; 29: 2065-2076.

35. Eftimie E. Linke turbidity factor for Braşov area. Bulletin of the Transilvania University of Braşov. 2009; 2: 61-68.

36. Ellouz F, Masmoudi M, Medhioub K. Study of the atmospheric turbidity over northern Tunisia. Renewable Energy. 2013; 51: 513-517.

37. Trabelsi A, Saad M, Masmoudi M, Alfaro S. Atmospheric aerosols and their impact on surface solar irradiation in Kerkennah Islands (eastern Tunisia). Atmospheric Research. 2015; 161: 102-107.

38. Kasten F. A simple parameterization of the pyrheliometric formula for determining the Linke turbidity factor. Meteor Rundschau. 1980; 33: 124-127.

39. Kasten F. The Linke turbidity factor based on improved values of the integral Rayleigh optical thickness. Solar Energy. 1996; 56: 239-244.

40. Elshazly S. A study of Linke Turbidity Factor over Qena / Egypt. Advances in Atmospheric Sciences. 1996; 13: 519-532.

41. Michaelides S, Evripidou P, Kallos G. Monitoring and predicting Saharan Desert dust events in the eastern Mediterranea. Weather. 1999; 54: 359-365.